Cycling-enhanced Knee Exoskeleton Using Planar Spiral Spring

Ronnapee Chaichaowarat, Jun Kinugawa, and Kazuhiro Kosuge, *Fellow, IEEE*

***Abstract*—Reported in our previous study on passive cycling support, the energy cost of knee extension can be reduced using the energy stored from knee flexion by torsion spring. In the current study, the planar spiral spring is applied to attain the compact design of the cycling augmented knee exoskeleton (CAKE-2). The surface electromyography (EMG) results over the rectus femoris muscles of three healthy male participants performing constant power cycling on a trainer at 200 W and 225 W are analyzed in time–frequency via the continuous wavelet transform. In all cycling tests with and without the exoskeletons worn on both legs, no sign of peripheral muscle fatigue or significant change in the EMG median power spectral frequency (MDF) appears throughout the two-minute cycling trials. At the same cycling speed and leg cadence, the average of EMG-MDF increases with the exercise intensity. At the same cycling power, less quadriceps activity can be observed from all the participants when the spring support was used during cycling. The capability to modify the unbalanced effort required from the quadriceps and the hamstring during cycling without requiring an external energy source is applicable for cycling enhancement and rehabilitation applications.**

I. Introduction

First introduced in the nineteenth century, bicycling is a classic activity enjoyed by billions of people worldwide for the purposes of recreation and sport. Cycling is eco-friendly and is also considered the most cost effective and time efficient means of transport for short to moderate distances. With the recent increase in global health awareness, people of all ages regularly perform this low-impact exercise to improve their cardiovascular endurance. Providing an effective closed kinetic chain (CKC) movement [1], cycling is widely used as a rehabilitation exercise for recovering knee-joint mobility and stability after a knee injury or surgery [2].

To improve the cycling performance and prevent bicycle-related injuries, the biomechanics of cycling was studied via the measurement of pedal force and leg kinematics [3] [4]. Figure 1 shows the unbalanced effort required from the quadriceps (knee extensor) and the hamstring (knee flexor), in which the maximum knee extension moment is up to three times that of the knee flexion moment in the uphill standing condition. The leg muscle activities throughout a crank cycle were studied from the surface electromyography (EMG) [5] [6]. The active duration of the rectus femoris and the vastii muscle is almost twice that of the hamstring [7]. Reducing the energy cost of knee extension was proposed as our strategy for cycling enhancement [8], with the aim to boost the riding duration and distance by maintaining the original road feeling and handling characteristics.

J. Kinugawa and K. Kosuge are with the Department of Robotics, Tohoku University, Sendai, Japan (kinugawa@irs.mech.tohoku.ac.jp, kosuge@m.tohoku.ac.jp).

R. Chaichaowarat is a doctoral student of the Department of Robotics, Tohoku University, Sendai, Japan (ronnapee@irs.mech.tohoku.ac.jp).

Considering general riders as the typical users, a compact passive wearable support is the best solution for adaptability and safety. By manipulating energy wisely, some passive [9] [10] and quasi-passive [11] exoskeletons using mechanical springs were proposed for various human support applications. For cycling, we developed the cycling augmented knee exoskeleton prototype, termed as CAKE-1 [8]. Concerning the kinematic compatibility with the anatomical knee joint, the crossing four-bar linkage [12] corresponding with the quadratic equations [13] obtained from [14] is still used in this CAKE-2 prototype. However, the planar rotary spring [15] is considered such that a higher torsional stiffness knee joint with a more compact structure can be achieved.

For the case of repetitive maximum dynamic knee extension [16], the decrease in the EMG mean power spectral frequency (MNF) over the time of contractions is related to the force decrease due to the progression of localized muscle fatigue. However, no significant signs of muscle fatigue appeared in the 30-min cycling test on an ergometer [17], because the decrement in the instantaneous MNF is very small. To study the change in the EMG power spectrum over the time of contractions [18], the signal can be analyzed in time–frequency via the continuous wavelet transform (CWT). Critical as a knee extensor muscle in the power stroke of cycling [19] [20], the rectus femoris (RF) is primarily selected in this work for the study of muscle activity change under the influence of torsion spring support.

Herein, the torsional stiffness and operating range of the passive cycling support are reconsidered for CAKE-2. A new design method for a planar spiral spring is proposed. The exoskeleton prototype using the new planar spiral spring is developed and evaluated through constant power cycling tests on a trainer. To avoid the effect of electrode–skin impedance imbalance in repetitive dynamic contractions, the average of the EMG median power spectral frequency (MDF) throughout the exercise interval has been proven effective as a new quantitative index representing the level of muscle activity.

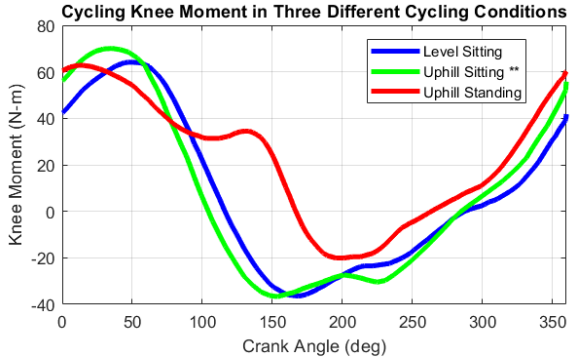

Figure 1. Knee moments corresponding to three cycling conditions: level sitting, uphill sitting, and uphill standing, as adapted from [4]. The crank angle starts at the pedal crank top dead center (TDC). The positive moment refers to the knee extension, and vice versa.

978-1-5386-3646-6/18/$31.00 ©2018 IEEE

Authorized licensed use limited to: PORTLAND STATE UNIVERSITY LIBRARY. Downloaded on February 21,2024 at 05:30:12 UTC from IEEE Xplore. Restrictions apply.

This paper is organized as follows: Section II explains the concept of passive cycling support, section III describes the design method for the planar spiral spring, section IV reveals the CAKE-2 prototype, section V shows the experimental setup and testing procedures, section VI discusses the results, and section VII summarizes the key findings.

II. Concept of Passive Cycling Support

A. Supporting Knee-extension Moment by Torsion Spring

From the study of cycling biomechanics [4], the knee angle and the (original) knee moment varying in a pedal crank cycle are respectively shown in Fig. 2(a) and Fig. 2(b). Taking advantage of the unbalanced effort on the knee extension and flexion, the cycling augmented knee exoskeleton (CAKE-1) [8] was designed to store energy from the knee flexion to release it as a supporting knee-extension moment. The knee joint power required to store the energy is much less than the average knee-joint power throughout the cycle.

Considering a torsion spring stiffness k_θ activating when the knee angle θ_K is larger than the starting angle θ_{K0}, the supporting knee moment τ_{Kspr} varying with the knee angle is written as (1). Assuming no human–device interfacing loss, the resultant knee moment τ_{Kres} required from the leg muscle with support can be predicted from the original knee moment τ_{Korg} and the supporting knee moment τ_{Kspr}, via (2).

$$\tau_{Kspr} = \begin{cases} k_\theta(\theta_K - \theta_{K0}) & , \ \theta_K \geq \theta_{K0} \\ 0 & , \ \theta_K < \theta_{K0} \end{cases} \quad (1)$$

$$\tau_{Kres} = \tau_{Korg} - \tau_{Kspr} \quad (2)$$

From the 0.25 N·m/° torsional stiffness around the knee joint with the 55° starting angle of CAKE-1, the supporting and the resultant knee moments obtained via (1) and (2), respectively, are shown with the original knee moment in Fig. 2(b).

B. Influence of Torsional Stiffness and Operating Range

Affecting the assistive performance of the passive cycling support, the torsional stiffness around the knee joint and the starting angle indicating the operating range are reconsidered for CAKE-2. By applying a 0.375 N·m/° stiffness with a 60° starting angle, the corresponding plots of the supporting and the resultant knee moments are also shown in Fig. 2(b). Plotted against the pedal crank angle, the slope of the supporting knee moment is related to but does not directly refer to the torsional stiffness. Assuming that the cycling knee angle does not change with the torsion spring support, the starting angle is carefully chosen such that the operating range of the support encompasses the pedal crank interval, in which the knee-extension effort is highly required.

To clarify the consequence of the energy manipulation performed by the passive cycling support, the supporting and the resultant knee moments corresponding to the CAKE-1 and CAKE-2 supports are plotted against the cycling knee angle in Fig. 3(a). Without and with the supports, the knee joint works: extension work, flexion work, and total work, obtained from the area under the curve of the original and the resultant knee moments, are compared in Fig. 3(b). With the fully-passive cycling supports, the total knee joint work is conserved in both configurations whereas the knee-flexion work is increased to tradeoff with the reduction in the knee-extension work.

According to the definition of effort over time (EoT) [8], the energy cost of knee extension, knee flexion, and the total energy cost can be obtained from the area under the curve of the original and the resultant knee moments plotted against the cycling time in Fig. 2(b), as compared in Fig. 3(c). With the supports, the energy cost of knee flexion is increased slightly to tradeoff with the significant reduction in the energy cost of knee extension and the total energy cost, especially with the CAKE-2 configuration.

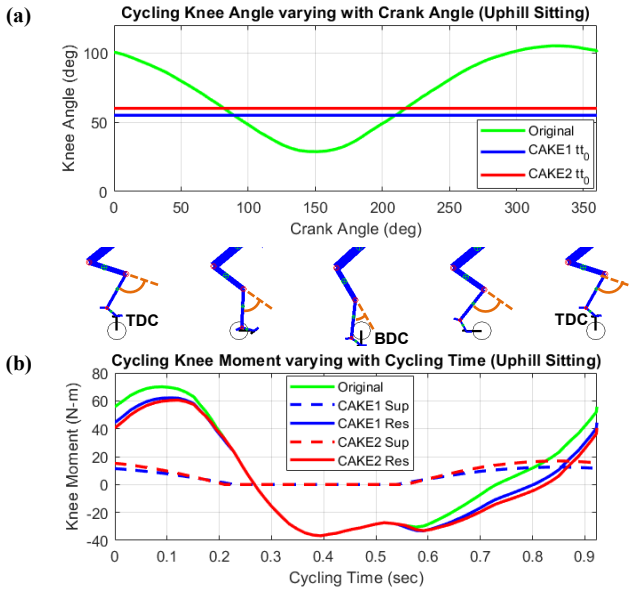

Figure 2. Knee angle varying with the pedal crank angle *(a)* and the (original) knee moment varying with cycling time *(b)*, as adapted from the uphill sitting condition [4]. Using the configurations of CAKE-1 and CAKE-2, the starting angles are shown in the angle plot *(a)*. The supporting and resultant knee moments are shown in the moment plot *(b)* where the positive moment refers to the knee extension, and vice versa.

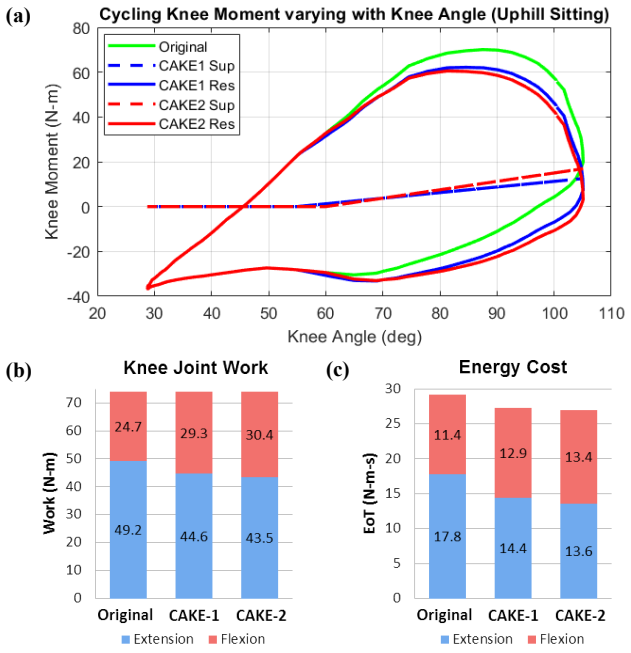

Figure 3. Original knee moment, the supporting and the resultant knee moments corresponding to the configurations of CAKE-1 and CAKE-2 shown against the cycling knee angle. *(a)* Knee joint works: extension work, flexion work and total work. *(b)* Energy cost of knee extension, knee flexion, and the total energy cost. *(c)*

Authorized licensed use limited to: PORTLAND STATE UNIVERSITY LIBRARY. Downloaded on February 21,2024 at 05:30:12 UTC from IEEE Xplore. Restrictions apply.

III. Design Method for Planar Spiral Spring

To attain a higher torsion stiffness knee joint with a more compact structure in CAKE-2, the custom torsion spring used in the previous prototype is replaced by the planar spiral spring. This type of spring design was widely used in series elastic actuators such as in [21]–[23]. The analytical model based on the curved beam theory was also proposed [24] for design optimization. Regarding the design formula of the spiral torsion springs from the handbook of spring design [25], the design procedure to accomplish the desired torsional stiffness and operating range is described in this section.

For a desired maximum torque M, the material width b and the spiral arm thickness t are selected such that the bending stress S, obtained from the deflecting beam formula (3), does not exceed the cyclic fatigue strength. The length of the active material L is computed by (4), from the modulus of elasticity E and a desired maximum angular deflection θ measured in revolutions. As the arbor diameter A is typically set first, the outer diameter in the free condition OD_F can be approximated from (5), to be used as a minimum allowance for preventing a tight wound-up spring on the arbor before the desired deflection is attained.

$$S = \frac{6M}{bt^2} \tag{3}$$

$$M = \frac{\pi E b t^3 \theta}{6L} \tag{4}$$

$$OD_F = \frac{2L}{\pi\left(\frac{\sqrt{A^2+1.27Lt}-A}{2t}-\theta\right)} - A \tag{5}$$

When a large outer diameter is required for the desired range of angular deflection, decreasing the spring arm thickness is a possible method to attain a compact shape of the spiral spring. However, the material width must be increased to maintain the desired stiffness.

For the geometry design, the arbitrary outer diameter OD is defined based on the minimum allowance. The spring arm is shaped from the Archimedean spiral, the polar coordinates (r, ϕ) of which are described by (6). The coefficients c_2 and c_1 are respectively obtained via (7) and (8), from the angle indicating the origin ϕ_0 and the total angle $\Delta\phi$ of the spiral arm. By trial and error, the total angle of the spiral arm is determined such that the length of the spiral arm L_ϕ, computed from (9), is equal to the length of the active material obtained earlier from (4).

$$r = c_1 + c_2\phi \tag{6}$$

$$c_2 = \left(\frac{OD}{2} - \frac{A}{2}\right)/\Delta\phi \tag{7}$$

$$c_1 = \frac{A}{2} - c_2\phi_0 \tag{8}$$

$$L_\phi = \int_{\phi_0}^{\phi_0+\Delta\phi} r\, d\phi \tag{9}$$

For the 34-mm arbor and 60-mm outer diameters, the length of the active material is satisfied by the total angle of the spiral arm = 5π rad, as the Archimedean spiral shown in Fig. 4(a).

By applying the obtained geometry design on the 5-mm AISI 302 stainless steel sheet, the 0.187 N·m/° stiffness with 60° maximum deflection can be achieved. The planar spiral spring of CAKE-2 is manufactured from the wire-cut-type electrical discharge machining (EDM), as shown in Fig. 4(b).

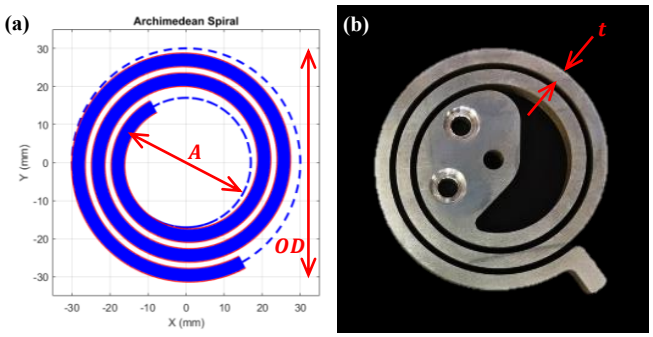

Figure 4. Geometry design of the spring arm based on the Archimedean spiral. *(a)* Planar spiral spring by EDM for the CAKE-2 prototype *(b)*

IV. Cycling-Augmented Knee Exoskeleton

Regarding the energy cost reduction, the assistive performance achieved from the CAKE-2 configuration over that of the CAKE-1 was previously demonstrated through theoretical simulations, as described in section II. For the experimental evaluation and for studying the leg muscle activity under the influence of the passive cycling support, the prototype of CAKE-2 is developed as shown in Fig. 5(a). Obtained from the Breg X2K knee brace (Breg, Inc.), the upper and lower wearable parts along with the fastened straps are applied in our prototype to ease the design and fabrication because extensive knowledge is required for the development of a comfort knee brace with high wearing firmness.

Concerning the kinematic compatibility with the anatomical knee joint, the identical configuration of the crossing four-bar linkage [12], providing a polycentric knee center of rotation is considered. The dual-hinge mechanism originally applied on the medial and lateral knee joints of the Breg X2K is replaced by the CAKE-2 knee-joint mechanism using a crossing four-bar linkage with planar spiral spring, as shown in Fig. 5(b). While flexing the knee to the starting angle, the spiral spring arm attached on the thigh leg will start applying the contact force to the stopper pin attached on the shank leg. Consequently, the supporting knee extension moment is generated. Two pieces of equal-stiffness (0.187 N·m/°) planar spiral springs are installed on both sides of the knee to provide the required torsional stiffness, significantly increased in this prototype with a more compact and light weight design.

For comparison, the specifications of both the CAKE-1 and CAKE-2 prototypes are summarized in Table 1. The knee flexion is considered to be in the same range from 0–120° in both designs. In CAKE-2, the total stiffness around the knee joint is deliberately increased to 0.375 N·m/° with the starting angle slightly retarded to 60° of the knee flexion. The total mass is successfully reduced from 1070 g to 700 g. To avoid obstructing with the top tube of a bicycle frame, the additional width of the medial mechanism is significantly decreased from 35 mm to only 20 mm, as shown in Fig. 6.

TABLE I. Specifications of the CAKE-1 and CAKE-2

Specification	*CAKE-1*	*CAKE-2*	*Unit*
Range of knee flexion	0–120		°
Total stiffness around knee joint	0.25	0.37	N·m/°
Starting angle of the support	55	60	°
Total mass	1070	700	g
Width of the medial mechanism	35	20	mm

Authorized licensed use limited to: PORTLAND STATE UNIVERSITY LIBRARY. Downloaded on February 21,2024 at 05:30:12 UTC from IEEE Xplore. Restrictions apply.

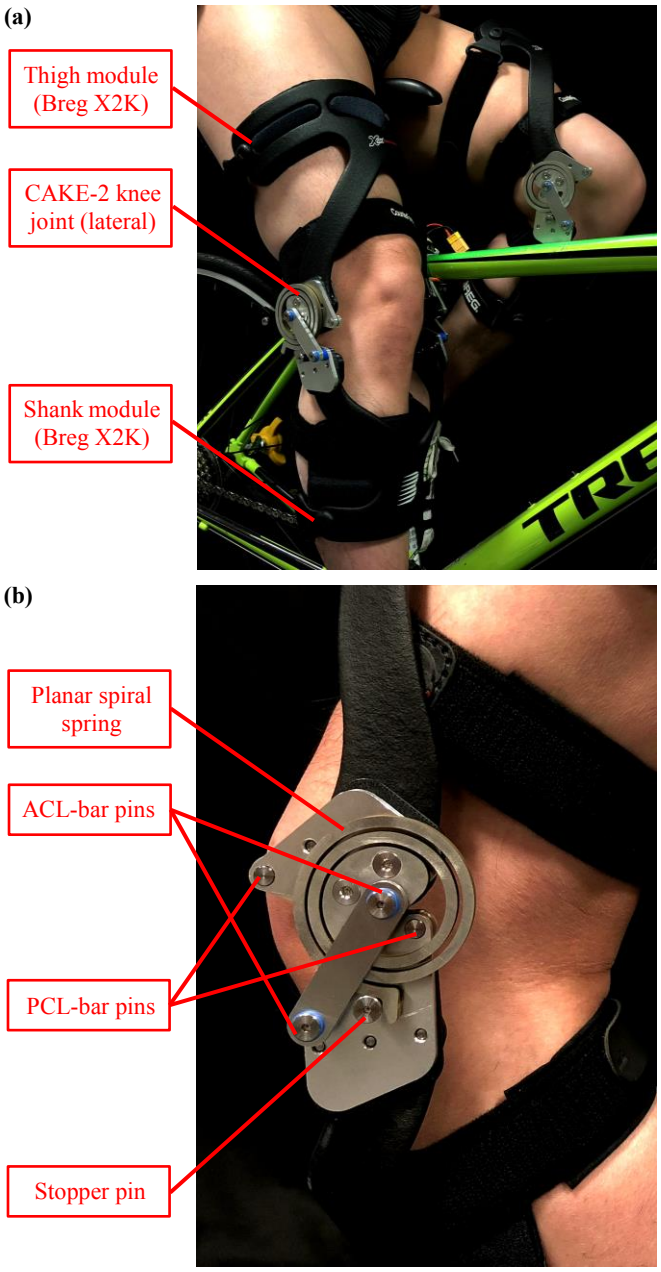

Figure 5. Feature and component of the CAKE-2 prototype during riding. *(a)* CAKE-2 knee-joint mechanism using a crossing four-bar linkage with planar spiral spring. *(b)*

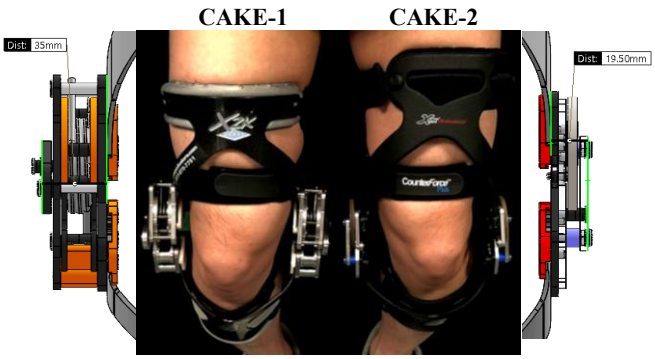

Figure 6. Front view picture of the CAKE-1 and CAKE-2 prototypes and CAD-rendered picture showing the width of the medial (or lateral) mechanism.

V. Experimental Setup

A. Experimental Environment

For studying the influences of cycling power and passive cycling support on the quadriceps femoris activity, an indoor stationary cycling environment is prepared, as shown in Fig. 7. A testing bicycle is mounted on a magnetic cycling trainer. The real-time monitoring of the cycling speed and leg cadence are provided by a bicycle speedometer. Developed from the previous study, the friction-drive wheel accelerating system is used to provide an initial spinning of the rear wheel to reach the target velocity of 30 km/h corresponding to the 200 W and 225 W cycling powers imparted by the road and the interval modes of the cycling trainer, respectively. On both legs of the participants, the dry-type surface EMG electrodes (Logical Product) are placed over the rectus femoris (RF) muscles to measure the EMG signal with 1-kHz sampling frequency.

B. Experimental Procedure

By assuming that the quadriceps activity increases with the cycling load under the controlled leg cadence, the influence of muscle activity increment on the surface EMG power spectral component is studied through the different power cycling tests performed by three healthy male participants, the information of which is summarized in Table 2. In each experiment, a participant is required to perform a 2-min warm up by the 225-W cycling on a trainer at 30 km/h and 57-rpm leg cadence. After placing the surface EMG electrodes over the RF muscles during the 10-min rest, the participant is required to perform the 2-min cycling trials for four times: at 225 W while wearing CAKE-2, at 225 W while wearing CAKE-1, at 225 W with free legs, and at 200 W with free legs. Separated by a 10-min break between each trial, all the cycling trials were performed at the same cycling speed (30 km/h) and leg cadence (57 rpm).

TABLE II. Participant Information for Cycling Experiment

Participant Information	*Average*	*SD*	*Unit*
Age	24.3	2.6	years
Height	172.7	3.1	cm
Weight	67.0	4.9	kg
Weekly cycling	320	57	min

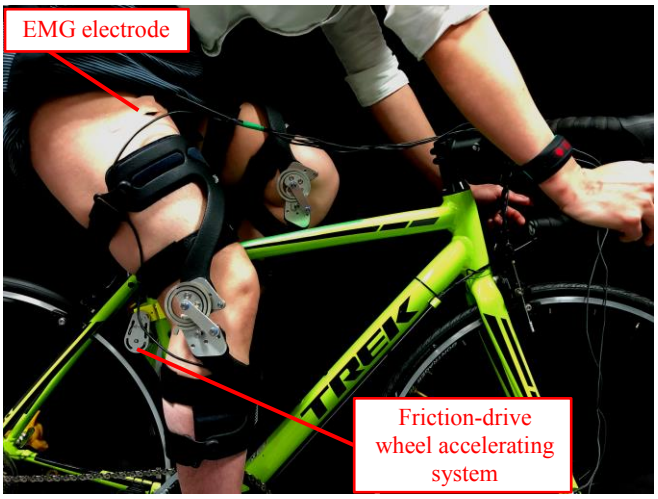

Figure 7. Indoor cycling experimental environment.

Authorized licensed use limited to: PORTLAND STATE UNIVERSITY LIBRARY. Downloaded on February 21,2024 at 05:30:12 UTC from IEEE Xplore. Restrictions apply.

VI. Results and Discussion

A. Root-mean-square EMG

Recorded at a 1-kHz sampling frequency, the surface EMG data obtained from the cycling experiment consists of the raw EMG measured in volts, and the root-mean-square (rms) EMG. Collected from 90-s interval of constant power cycling, the rms EMG of the RF muscle corresponding to the right leg of participant-1 and the left leg of participant-2 are respectively shown in Fig. 8 (a-1) and Fig. 8 (b-1). According to the 10-s enlarged plots of both participants, shown in Fig. 8 (a-2) and Fig. 8 (b-2), the decrease in the rms EMG with the cycling power is shown by comparing the results of the cycling trials without wearing the support (Leg-225 and Leg-200).

By cycling at 225 W with the CAKE-2 or CAKE-1 support (Ex2-225 or Ex1-225), the rms EMG can be reduced to nearly the same level as the 200-W cycling without wearing the support (Leg-200). However, the advantage of the newly developed prototype CAKE-2 over the previous prototype CAKE-1 in terms of RF muscle activity reduction still cannot be verified based on the rms EMG results.

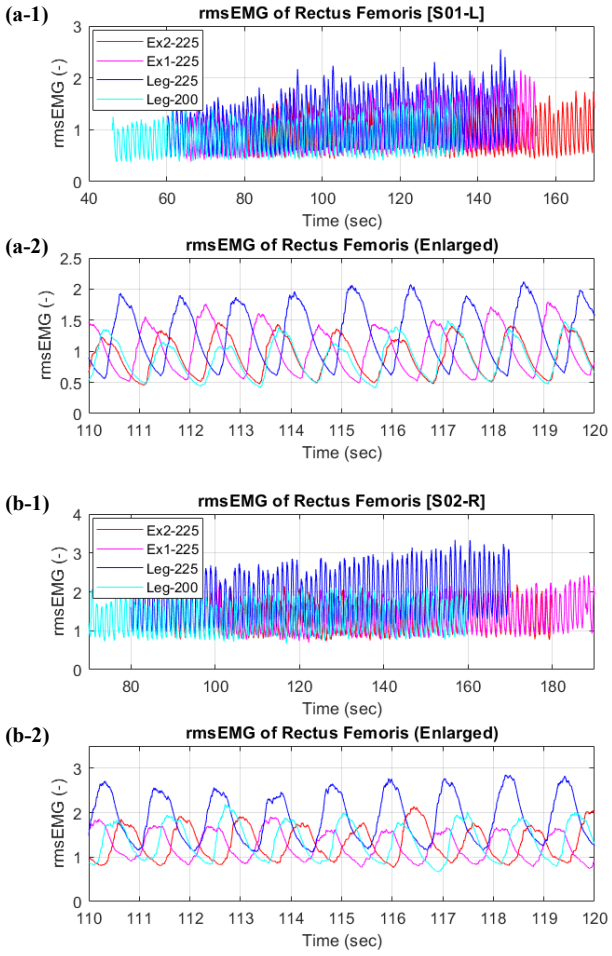

Figure 8. RF muscle root-mean-square EMG: right leg of participant-1 *(a)* and left leg of participant-2 *(b)*. The upper plots: *(a-1)* and *(b-1)* show the rms EMG over a 90-s interval. The lower plots: *(a-2)* and *(b-2)* show only a 10-s interval with the enlarged scale. The rms EMG from the 225-W cycling with CAKE-2 and CAKE-1 are denoted by "Ex2-225" and "Ex1-225," respectively. The rms EMG from the free-leg cycling at 225 W and 200 W are denoted by "Leg-225" and "Leg-200," respectively.

B. EMG Time–Frequency Analysis

To eliminate the sensing noise, the raw EMG data of each individual muscle is first processed through a low-pass FIR filter with 110-Hz cut-off frequency. Subsequently, the filtered EMG data is analyzed in time–frequency via the CWT. Combining the wavelet transform coefficients corresponding with the right and the left leg rectus femoris muscles of each participant, the time–frequency plot showing the EMG power spectrum change over the 90-s cycling interval is obtained for each cycling test condition.

The time–frequency plots obtained from the 225-W cycling performed by participant-3, with and without wearing the CAKE-2 support are respectively shown in Fig. 9(a) and Fig. 9(b). In each plot, the instantaneous EMG median power spectral frequency (EMG-MDF) along with the linear regression line is shown. Over the 90-s interval, no sign of peripheral muscle fatigue is observed through the significant change in the EMG-MDF. Comparing the average value of the EMG-MDF obtained from both cycling trials, the averaged EMG-MDF of the cycling test with the CAKE-2 support is slightly lower than that of the cycling test without wearing the support.

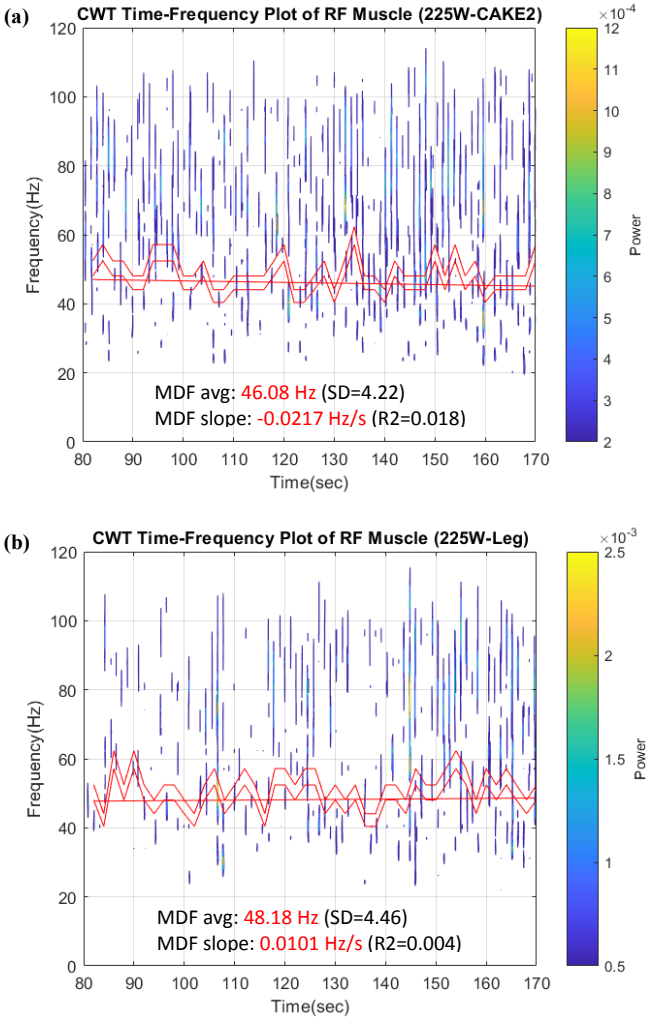

Figure 9. CWT time–frequency plots of RF muscle (both legs) observed from the 225-W cycling trials performed by participant-3, with wearing CAKE-2 *(a)* and without wearing any support (leg) *(b)*.

Authorized licensed use limited to: PORTLAND STATE UNIVERSITY LIBRARY. Downloaded on February 21,2024 at 05:30:12 UTC from IEEE Xplore. Restrictions apply.

For comparison, the average value of the EMG median power spectral frequency over 90-s for all cycling trials performed by all the three participants are presented in Fig. 10. In the cycling trials without wearing the support (225-W leg vs. 200-W leg), the lower averaged EMG-MDF can be observed with the lower cycling power from all the participants. With the passive cycling supports (225-W CAKE-2 and 225-W CAKE-1), the averaged EMG-MDF can significantly be reduced in comparison with the cycling without wearing the support (225-W leg and 200-W leg). Regarding the decrease in the averaged EMG-MDF that reflect the reduction in the RF muscle activity, the advantage of the newly developed CAKE-2 over the previous CAKE-1 prototype is demonstrated from the results corresponding to participant-1 and participant-2.

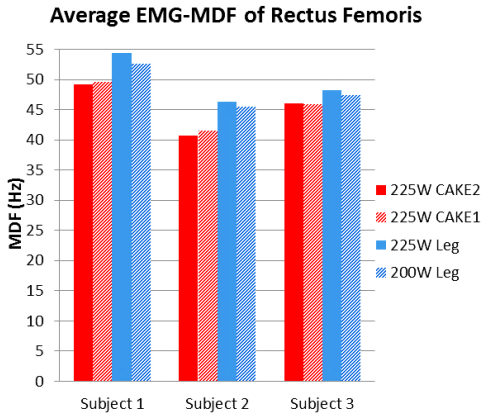

Figure 10. Summary of the average EMG median power spectral frequency corresponding to the 225-W cycling with CAKE-2 and CAKE-1 and the free-leg cycling without the supports at 225 W and 200 W.

VII. Conclusion

The capability to modify the unbalanced effort required from the quadriceps and the hamstring during cycling without requiring external energy sources can be applied for cycling enhancement and rehabilitation applications. Because of the fastened strap locations, the study of the hamstring muscle activity is limited in this study. Considering the effect on oxygen consumption or metabolic energy is also important for future studies.

The proposed design method of the planar spiral spring is applicable for various uses. Because the CAKE-2 prototype was developed and validated through stationary cycling tests, the dynamic advantage due to the weight reduction over the previous prototype is not discovered. The CAKE concept will be further explored to attain a more user-friendly wearable device with reasonable production cost.

From our study, the lower EMG-MDF is related to the lower muscle activity. Therefore, the proposed EMG-MDF concept can be used as an alternative method to compare the level of muscle activity in other dynamic exercise activities.

References

[1] E. B. Bynum, R. L. Barrack, and A. H. Alexander, "Open versus closed chain kinetic exercises after anterior cruciate ligament reconstruction. A prospective randomized study," *Am. J. Sports Med.*, vol. 23, no. 4, pp. 401–406, 1995.

[2] W. D. McLeod and T. A. Blackburn, "Biomechanics of knee rehabilitation with cycling," *Am. J. Sports Med.*, vol. 8, no. 3, pp. 175–180, 1980.

[3] M. L. Hull and M. Jorge, "A method for biomechanical analysis of bicycle pedaling," *J. Biomech.*, vol. 18, no. 9, pp. 631–644, 1985.

[4] G. E. Caldwell, J. M. Hagberg, S. D. McCole, and L. Li, "Lower extremity joint moments during uphill cycling," *J. Appl. Biomech.*, vol. 18, pp. 166–181, 1999.

[5] M. Jorge and M. L. Hull, "Analysis of EMG measurements during bicycle pedalling," *J. Biomech.*, vol. 19, no. 9, pp. 683–694, 1986.

[6] L. Li and G. E. Caldwell, "Muscle coordination in cycling: effect of surface incline and posture," *J. Appl. Physiol.*, vol. 85, no. 3, pp. 927–934, 1998.

[7] S. J. Houtz and F. J. Fischer, "An analysis of muscle action and joint excursion during exercise on a stationary bicycle," *J. Bone. Joint Surg.*, vol. 41(A), pp. 123–131, 1959.

[8] R. Chaichaowarat, D. F. Paez G., J. Kinugawa, and K. Kosuge, "Passive knee exoskeleton using torsion spring for cycling assistance," in *Proc. 2017 IEEE/RSJ Int. Conf. Intelligent Robots and Systems*, pp. 3069–3074.

[9] A. N. Spring, J. Kofman, and E. D. Lemaire, "Design and evaluation of an orthotic knee-extension assist," *IEEE Trans. Neural Syst. Rehabil. Eng.*, vol. 20, no. 5, pp. 678–687, 2012.

[10] S. H. Collins, M. B. Wiggin, and G. S. Sawicki, "Reducing the energy cost of human walking using an unpowered exoskeleton," *Nature*, vol. 522, no. 11, pp. 212–215, 2015.

[11] A. M. Dolla and H. Herr, "Design of a quasi-passive knee exoskeleton to assist running," in *Proc. 2008 IEEE/RSJ Int. Conf. Intelligent Robots and Systems*, pp. 747–754.

[12] J. M. Baydal B, et al., "Development of a hinge compatible with the kinematics of the knee joint," *Prosthet. Orthot. Int.*, vol. 31, no. 4, pp. 371–383, 2007.

[13] P. S. Walker, H. Kurosawa, J. S. Rovick, and R. A. Zimmerman, "External knee joint design based on normal motion," *J. Rehabil. Res. Dev.*, vol. 22, no. 1, pp. 9–22, 1985.

[14] H. Kurosawa, P. S. Walker, S. Abe, A. Garg, and T. Hunter, "Geometry and motion of the knee for implant and orthotic design," *J. Biomech.*, vol. 18, no. 7, pp. 487–499, 1985.

[15] N. Georgiev and J. Burdick, "Design and analysis of planar rotary springs," in *Proc. 2017 IEEE/RSJ Int. Conf. Intelligent Robots and Systems*, pp. 4777–4784.

[16] J. S. Karlsson, N. Ostlund, B. Larsson, and B. Gerdle, "An estimation of the influence of force decrease on the mean power spectral frequency shift of the EMG during repetitive maximum dynamic knee extensions," *J. Electromyogr. Kinesiol.*, vol. 13, pp. 461–468, 2003.

[17] M. Knaflitz and F. Molinari, "Assessment of muscle fatigue during biking," *IEEE Trans. Neural Syst. Rehabil. Eng.*, vol. 11, no. 1, pp. 17–23, 2003.

[18] J. L. Dantas, et al., "Furrier and wavelet spectral analysis of EMG signals in isometric and dynamic maximal effort exercise," in *Proc. 2010 IEEE/EMBS Annu. Int. Conf.*, pp. 5979–5982.

[19] C. A. Wozniak T., "Cycling biomechanics: a literature review," *J. Orthop. Sports Phys. Ther.*, vol. 11, no. 3, pp. 106–113, 1991.

[20] M. O. Ericson, R. Nisell, U. P. Arborelius, and J. Ekholm, "Muscular activity during ergometer cycling," *Scand. J. Rehab. Med.*, vol. 17, pp. 53–61, 1985.

[21] B. Knox, J. Schmiedeler, "A unidirectional series-elastic actuators design using a spiral torsion spring," *J. Mech. Design*, vol. 131, 2009.

[22] A. Stienen, et al., "Design of a rotational hydroelastic actuator for a power exoskeleton for upper limb rehabilitation," *IEEE Trans. Biomed. Eng.*, vol. 57, no. 3, 2010.

[23] C. Lagoda, A. Schouten, A. Stienen, E. Hekman, and H. Kooij, "Design of an electric series elastic actuated joint for robotic gait rehabilitation training," in *Proc. 2010 IEEE RAS/EMBS Int. Conf. Biomedical Robotics and Biomechatronics*, pp. 21–26.

[24] N. Georgiev and J. Burdick, "Design and analysis of planar rotary spring," in *Proc. 2017 IEEE/RSJ Int. Conf. Intelligent Robots and Systems*, pp. 4777–4784.

[25] P. Williams, *Handbook of spring design*. Spring Manufacturers Inst., PA: Pennsylvania State University, 1991.

Authorized licensed use limited to: PORTLAND STATE UNIVERSITY LIBRARY. Downloaded on February 21,2024 at 05:30:12 UTC from IEEE Xplore. Restrictions apply.